A Descriptive Geometry Construction of VR Panoramas in Cubical Spherical Perspective

António Bandeira Araújo, Lucas Fabián Olivero, Adriana Rossi

Abstract

Hand-drawn spherical perspectives are increasingly used as both a technical and artistic vehicle for representation of wide-angle views, partly due to their connection with VR panoramas. Recent results have made it easier to draw such perspectives in a systematic way in the equirectangular and azimuthal equidistant cases. In this paper we look at cubical perspective as a special case of a spherical perspective and describe a method to draw it systematically using simple descriptive geometry constructions, by classifying and rendering its geodesics.

Keywords: cubical perspective, spherical perspective, VR panoramas, descriptive geometry, geodesics.

Introduction

Architects and artists have always found it useful to draw wide angle views, both for information gathering and for visualization purposes. Information gathering today relies heavily on complex hardware and software, such as 360-degree photography [Cabezos Bernal, Cisneros Vivó 2016], 3D laser scanning, point clouds [Barba, Fiorillo, Naddeo 2014], etc., and immersive visualization can be achieved through VR panoramas of photographic data or rendering of 3D models [Rossi 2017, pp. 4-21]. These useful tools have their own pitfalls, as they can lead to black-box thinking [Araújo 2018b, p. 16], hence drawing, being a form of thinking through experimentation [Schön 2017, p. 159; Tran Luciani, Lundberg 2016, p. 1491] even more than a form of representation [García-García, Galán Serrano, Arce Martínez 2016, p. 1040], retains its importance. A drawing highlights the personal interpretation of reality in the eyes of the draughtman or his "conceptual model" [Arnheim 1954, pp. 2, 171]. VR panoramas allow for an interesting interaction between digital rendering and traditional drawing, as they can be generated by hand-drawn spherical perspectives.
Flocon and Barre [Barre, Flocon, Bouligand 1967] systematized the first ruler and compass construction of a spherical perspective (in fact only a hemi-spherical view), rendering the anterior hemisphere of an azimuthal equidistant map projection (the so called "fisheye" perspective, which allows for a 5-point-perspective). Their construction was extended to the full spherical view (a total spherical perspective, which allows for a 6-point-perspective) in a recent work [Araújo

2018a] that also provided a general mathematical schema for central curvilinear perspectives based on a redefinition of the notion of anamorphosis. This schema was later applied to solve the equirectangular perspective [Araújo 2018b] with a view to the hand-drawing of VR panoramas.
But if fisheye perspective has a special place among artists and equirectangular spherical perspective has an important practical status among programmers (being the standard format for VR panoramas), cubical perspective deserves special consideration among architects, engineers and artists, due to the simplicity of its line projections [Olivero, Sucurado 2019, pp. 54-57]. By cubical perspective we mean the flat image obtained by projecting a 3D environment conically onto a cube's surface and then flattening the cube. This has the advantage that the projection on each face is a classical perspective, or to be more precise, a plane anamorphosis with regard to the cube's centre. The difficulty lies in managing all six faces in an efficient way, obtaining all vanishing points and line images in an organized and systematic fashion. We will see that simply treating each face as a classical perspective is quite inefficient.
Cubical perspective has been lately investigated with partial results in recent works [Barba, Rossi, Olivero 2018, p. 33; Olivero, Rossi, Barba, 2019, p. 61]. The present work completes the full solution outlined in [Araújo, Olivero, Rossi 2019] by framing cubical perspective as a special case of the spherical perspective schema of [Araújo 2018a]. We argue that cubical perspective is better seen as a spherical perspective, and, as in all such perspectives, most easily solved by first classifying and rendering all images of spherical geodesics. This is what we do in the present work, achieving in this way its complete and systematic solution, that is, a method for systematic and complete construction of all lines images and vanishing points of a given scene, from both direct angular measurements or from architectural plans.

Towards a consistent and efficient method

Let's begin intuitively. Consider a station point O (the observer's eye) and around it place a cube with centre O. Project the 3D environment conically towards O and mark where each ray hits the cube. Now cut and flatten the cube. You get a picture like (fig. 1a). Locally, on each face, it looks like a classical perspective; every line projects to a line segment, and sets of parallels have at most one vanishing point; globally, however, lines are (sometimes disconnected) unions of segments, and all families of parallels have exactly two vanishing points. It was pointed out in [Barba, Rossi, Olivero 2018, p. 33] that it is quite hard, when a line crosses an edge of the cube, to know what angle it will make with the edge where it reappears.
The obvious solution is just to solve the individual classical perspectives of the cube faces the line projection touches. These are four at the most. This would require at least three points measurements for each pair of faces (fig. 1c). Not only is this inefficient, it creates a consistency problem when drawing from direct observation (unlike from plan and elevation), as each measurement of the visual angles (azimuth and elevation) will come with an independent random measurement error. The resulting object will not be a line but a union of segments, which will visibly change direction when seen immersively in the VR panorama (fig. 1c right).
We will solve all these problems by a different interpretation: we will regard a line as a subset of a geodesic and will determine the full geodesic image from just two points. This avoids the consistency problem, is maximally economic, and solves the angle problem automatically.

Cubical perspective

We begin by defining a cubical perspective. Given a point O in the 3-dimensional Euclidean space R^3, a cubical perspective with regard to O is a map from $R^3 \backslash O$ to a compact (i.e., bounded and closed) subset of the plane R^3 obtained in two steps: a conical projection towards the centre O of the cube, followed by a flattening of the cube onto a plane. Given a spatial point P, its conic projection is the intersection of ray OP with the cube's surface (fig. 1d left). We obtain the perspective image of P by flattening the cube. This flattening consists in cutting seven edges and rotating the faces around the remaining edges in such a way as to bring all faces onto the same plane. The projection is defined up to the choice of the cuts. We specify one such flattening: choose two arbitrary adjacent faces, denoted by F (for Front) and R (for Right). Denote the other faces L (left), B (back), U (up), D (down), in the order implied by this choice of relative directions. Name the edges by the faces they separate, so for instance FR is the edge between faces F and R. Then cutting edges UL, UB, UR, DL, DB, DR, BL we obtain the flattening of (fig. 1d right). Edges that are cut in the flattening appear twice in the drawing, so for instance point S appears on the edge UL on both faces U and L.

This procedure defines a perspective that behaves like a classical perspective in each projected face of the cube, but on the whole obtains a full 360-degree view of the environment around *O*. That is, an observer at *O*, looking from inside the cube at the conical projection of a spatial scene painted on the cube's surface would have the impression of seeing the actual spatial scene. This anamorphic effect can be reconstructed from a given cubical perspective by folding it back into a 3D cube. This is just what happens with VR visualization: the planar image is folded onto a virtual cube and the viewer interactively observes a flat anamorphosis (against the plane of the monitor) of the cubic anamorphosis specified by the perspective drawing. This allows us to go from an imaginary or observed flat drawing to an immersive environment (fig. 1b).

Immersive anamorphoses and spherical perspectives

We follow [Araújo 2018a, p. 149] in defining a spherical perspective as a central conical anamorphosis onto a sphere of centre *O*, followed by a flattening of the sphere that verifies certain continuity conditions. As explained in that work, the end result is a topological compactification of the spatial scene that preserves in the plane certain features of the spherical anamorphosis. We now recall some important properties of spherical anamorphosis:
A spatial line l determines a plane π through the centre *O* of the sphere. π defines, by intersection with the sphere, a great circle, or geodesic *g*. The anamorphic image of *l* is one half of *g* (a meridian). That meridian's endpoints are the two vanishing points of *l*, hence any line has exactly two such vanishing points. These are found by translating *l* to *O* and intersecting it with the sphere; hence the two vanishing points are antipodal to each other, i.e., diametrically opposite on the sphere. Given a spatial object, its perspective is the plane drawing obtained from its anamorphic projection by flattening the sphere itself onto the plane.
Now consider that the cube is homeomorphic to the sphere (fig. 1e) – the conic projection towards a centre *O* in common to a sphere and a cube defines a bijection between the two surfaces that is continuous both ways (a homeomorphism). So, the flattening of the cube defined in the previous section is also a flattening of the sphere. Hence cubical perspective is a special case of a spherical perspective. We can characterize it as the cubical spherical perspective.
Through this homeomorphism all concepts of spherical perspective, such as antipodal points or geodesics translate directly to the cubic case. In particular, two non-antipodal points on the cube's surface determine one single geodesic through them.
This means that if we have two points *P* and *Q* on two faces of the cube (fig. 1f), then there is a single correct way of connecting them that corresponds to a possible line segment between any two spatial points that project to *P* and *Q*. This will be part of a geodesic *g*. We also know that *g* must be made up of Euclidean line segments, as cubical perspective is a linear projection on each face.
In order to solve this perspective, we must show how to plot points from their angle measurements; plot antipodes; find vanishing points; classify and draw great circles. These are the common steps to the resolution of all spherical perspectives.

Solving the cubical perspective with descriptive geometry

We will see how to solve the cubical perspective through descriptive geometry constructions over the flattened cube. First some notation. We denote spatial points by bold font letters and both their conic projections onto the cube and their perspective projections onto the plane by the same letter in light font, unless context makes the distinction unclear. We call O_l to the centre of each face l of the flattened cube (for instance O_F for face *F*). This corresponds to the orthogonal projection of *O* onto each face. We say that faces *F*, *R*, *B*, *L* are horizontal faces and that *U* and *D* are vertical faces. This of course refers to relative bearings, not to absolute ones.

l - Antipodes
Let *P* be a point on the cube. We call antipode of *P* to its diametrically opposite point on the cube and denote it by P^-.
Construction l (antipode of a given point *P*): if *P* lies on face *l* then P^- lies on the opposite face, and by the opposite angles theorem, $\angle POO_l = \angle P^-OO_l^-$ (fig. 2a left). P^- can be obtained by a sequence of two transformations on the perspective view (fig. 2a right): first rotate *P* by 180° around the *z* axis, then reflect it across the plane of the horizon *H*. There are two cases: if *P* is on a horizontal face, then the rotation becomes a translation of two cube side lengths to the right (resp. left), if *P* is on faces *L* or *F* (resp. *R* or *B*). If *P* is on face *U* (resp. *D*), then translate *P* down (resp. up) by two side lengths and reflect across the vertical axis through O_F.

Fig. 1. L.F. Olivero, Introducing cubical perspective. a) Imaginary architecture; Scan QR code to see VR as in b); c) Representation of a line l: green segments from measured A, B, S don't align in VR; purple segments from measured A, B and calculated S, do; d) Flattening; e); Cube-sphere homeomorphism; f) Geodesic.

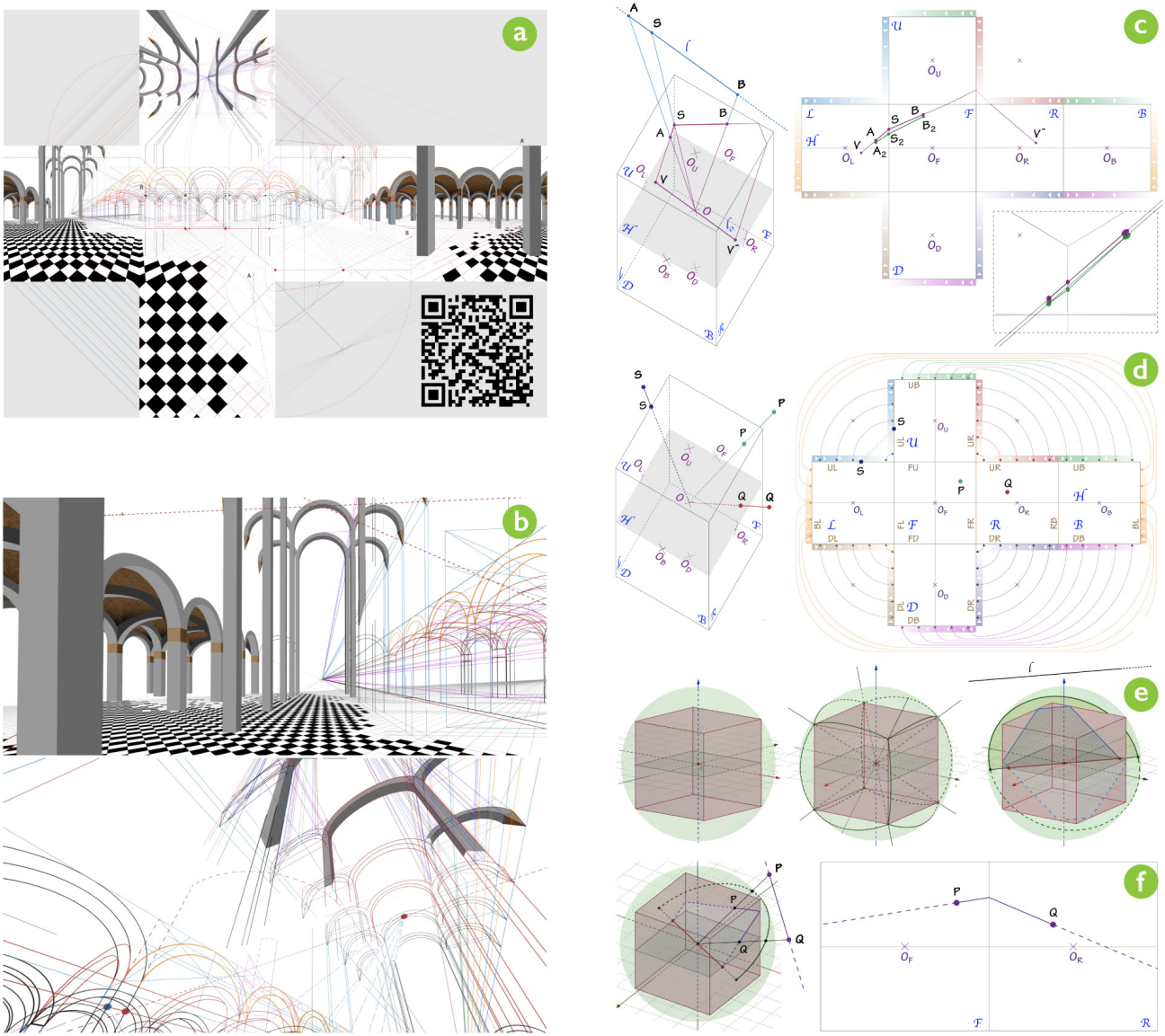

II - Construction of geodesics
We will now show how to obtain the images of spherical geodesics (great circles) on the cube surface and on the flat cubical perspective.
Two non-antipodal points *P* and *Q* on the cube's surface determine a plane $\pi=POQ$ through the centre of the cube and of its concentrical sphere, hence a spherical geodesic. The image of this plane on the cube is a set of connected line segments over the cube surface. We know this since on each face we have the intersection of two planes, hence a line segment. We know these must connect because this is a topological property and the cube is homeomorphic to the sphere. We also know this image must be either 4-sided or 6-sided since for each of its points on one face, there is an antipodal point on the opposite face, hence the number of faces is even, hence it is 4 or 6, since just 2 segments wouldn't connect.
We will now show the properties of the geodesic generated by two arbitrary points *P* and *Q*, according to the relative position of these points, and how to obtain its projection through descriptive geometry constructions. There are several cases to consider, and it is useful to start by isolating the properties of geodesics according to their number of sides.

II.1 4-Sided Geodesics
Suppose that a geodesic *g* contains a segment *l* on a face *l* such that *l* intersects two parallel edges of *l* at points *P* and *Q* respectively. Then P^- and Q^- are points of *g* on the respective antipodal edges of the face opposite to *l*. Segments P^-Q and PQ^- belong to *g* and are located on faces adjacent to *l* and opposite to each other. Joining their endpoints, we get a 4-sided closed loop, PQP^-Q^-, which is the full image of *g*. We call such loops 4-cycle (fig. 2b-2e).
When a *4-cycle* only touches the horizontal faces, we say it is *panoramic*. We say that a geodesic *g* is grid-like if projects on a face *l* as a segment *l* parallel to one of the edges e of that face. Then *l* intersects the two edges of *l* orthogonal to e in two points *P* and *Q*, hence P^-Q^- is the projection of *g* on the face opposite to *l*, and $g = PQP^-Q^-$ is a *4-cycle*. Also, by symmetry, QP^- and Q^-P pass through the centres of their respective faces. In (fig. 2e centre), *PQ* is directly passing through the centre of *l*, and therefore P^-Q^- will also do it in the opposite face. If *l* coincides with e, they are the diagonals of these faces (fig 2e right).
We note that if a geodesic crosses an edge at two points, then its plane contains the line that joins them, hence contains the whole edge, hence is *grid-like*. Then a *non-grid-like* geodesic only crosses an edge at one point at most.
Intuitively, *grid-like* geodesics are those generated by "horizontal" and "vertical" lines.

II.2 6-Sided Geodesics
Suppose a geodesic *g* contains a segment *l* that cuts adjacent edges of a face *l* at points *P* and *Q* (fig. 2f). Then let l_O be the line through *O* parallel to *l*. l_O intersects a face *J* adjacent to *l* at a point *M* that lies on the plane through *O* parallel to *l*. Either *P* or *Q* share a face with *M*. Suppose without loss of generality that it is *Q*. Then there is a point *N* on an edge adjacent to that of *Q* such that the image of *g* on *J* is *QN*. Then joining segments *PQ*, *QN*, NP^-, P^-Q^-, Q^-N^-, N^-P, we get a the *6-cycle* $g = PQNP^-Q^-N^-$ (fig. 2f-2i).

II.3 Descriptive Geometry construction of a geodesic through two given points
Given the perspective images of two points *A* and *B* which are not antipodal to each other, there is a single geodesic *g* through *A* and *B*. We will now use the classification above as a guide to draw the perspective image of *g* using descriptive geometry.
Case 1: Suppose *A* and *B* are on the same face *l*. Then line *AB* cuts the border of the face at two points *P* and *Q*. We must consider several sub-cases:
Case 1.1: *A* and *B* are such that *P* and *Q* are on opposite edges. We have described above the construction, from *P* and *Q*, that results in a *4-sided cycle*. We now show its descriptive geometry implementation according to the faces and edges involved.
Case 1.1.1: *P* and *Q* are on vertical edges of one of the horizontal faces. (fig. 2d) illustrates this case, assuming *A* and *B* on face *F* without loss of generality. Then P^- and Q^- found by *Construction 1*, are also on two further distinct vertical edges of this same set of faces. Further, due to edge identification, one of the antipodes (assume it is Q^-) will appear repeated in the drawing, on a further distinct vertical edge. Hence there are points on five vertical edges, that can be joined to obtain a *4-cycle* geodesic of the panoramic type.
Case 1.1.2: *P* and *Q* are on horizontal edges. If *P* and *Q* are on the horizontal edges of face *F* or *B* (fig. 2c) then P^- and Q^-, are on the horizontal edges of *B* or *F* (respectively). Then edge identification finds P^- and Q^- again on faces *U* and *D*. This gives a *4-cycle* that crosses only horizontal edges of *F*, *U*, *B*, *D*.
If *P* and *Q* are on one of the faces *L* or *R* (fig. 2d), then P^- and Q^- will be on the other. Without loss of generality, we can assume that *P* is on *LU* (resp. *RU*) and therefore *Q* is on *LD* (resp. *RD*). Then by edge identification, P^- is on *RD*

Fig. 2. L.F. Olivero, Antipodes and geodesics. a) Antipodes of points P,Q and S; b, c,d) Geodesics for P and Q on parallel edges; e) Examples of 4-cycle geodesics (central and right examples are grid-like); f) 6-cycle geodesic; g, h, i) Geodesics for P and Q on adjacent faces.

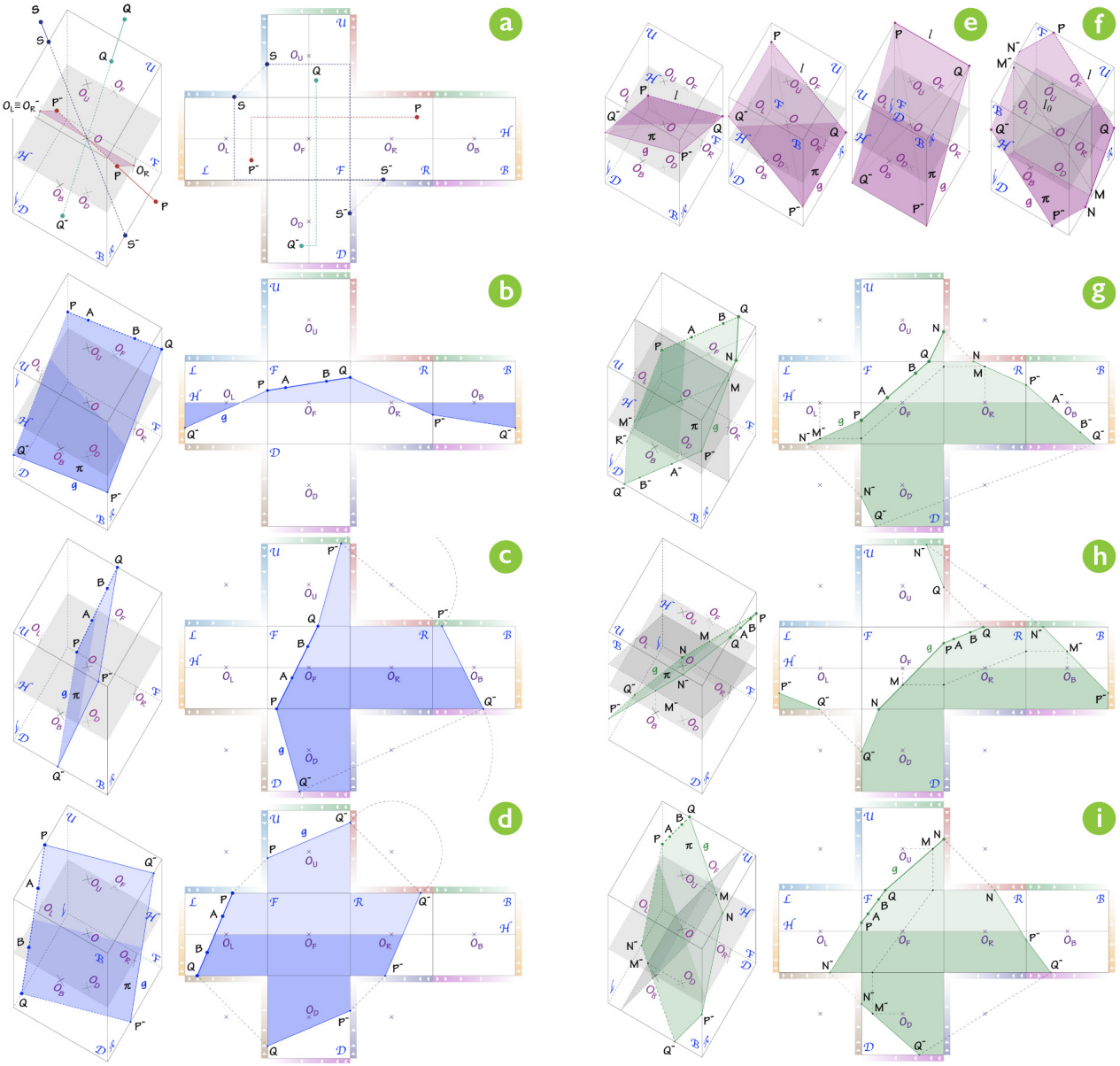

(resp. *LD*) and Q^- is on *RU* (resp. *UL*). Together, these points determine 4 segments on *L*, *U*, *R*, *D* that define a *4-cycle*. All the segments are disconnected on the plane.
Case 1.2: *A* and *B* are such that *P* and *Q* are on adjacent edges. We have seen above that this is a *6-cycle* constructed with the help of the auxiliary points *M* and *N*. We now construct these in the plane projection. To settle ideas, suppose that *A* and *B* are on face *F* and that *P* and *Q* are respectively on *LF* and *FU*, as in (fig. 2g). We obtain a further segment P^-Q^- on face *B* by taking antipodes and two further points, one on *U* and another on *D* by edge identification. We have seen above that we obtain two further points *M* and M^- in the geodesic by taking l_O, a parallel to *AB* through *O*, and intersecting it with the cube. Since *AB* is on *F*, that intersection must lie at the plane parallel to *F* through *O*, hence its plane projections must lie at the vertical lines through the centre of faces *L* and *R*, or at the horizontal lines through the centres of faces *U* and *D*. Then to obtain *M*, we take a parallel to *AB* through O_F. It must touch either the two vertical or the two horizontal edges of *F*. For concreteness suppose it intersects the verticals. Pass a horizontal line through the intersection on *FR* and intersect it with the vertical through O_R to obtain *M*. Draw a line P^-M and intersect it with *UR* to find point *N*. Taking an antipode, we find N^- on *DL*. We now have a segment in each face and a complete *6-cycle*. The choices we made do not lead to loss of generality, as we can obtain all other cases by reflection through the vertical or horizontal line through the centre of *O*, or by cyclical translation of the face where *A* and *B* lie (figs. 2g-2i).
Case 2: Suppose *A* and *B* are points on faces adjacent to each other. In this situation we can have either a *4-cycle* or a *6-cycle*, depending on the relative positions of the given points. We need an auxiliary point to determine the geodesic through *A* and *B*. Let *e* be the common edge of faces F_A and F_B where *A* and *B* are located (fig. 3a). Let $\pi = AOB$ be the plane of the geodesic determined by these points. Then segment *AB* is in π. Let δ_e be the plane through *O* and e. Then *AB* intersects δ_e at a point *C*. Since *C* is in *AB*, hence in π, then the ray *OC* is in π. Let l_e be the line that contains edge e. Ray *OC* intersects l_e at some point *S*, also in π. Then lines *AS* and *BS* will determine the images of the plane π in the faces F_A and F_B.
We now show how to construct the auxiliary point *S* through a descriptive geometry diagram. We take edge e as a folding line so as to draw F_A and F_B on the same plane (fig. 3b). On the same drawing we consider a top view of the two faces, i.e., an orthogonal projection over a plane ε perpendicular to e. On ε, e projects as point E_ε and faces F_A and F_B form two adjacent sides of a square. We draw ε so that the image of F_A on it coincides with the bottom edge of F_A. The projection O_ε of *O* on ε is at the centre of the square defined by F_A and F_B, δ_e is a diagonal through O_ε and E_ε, with A_ε and B_ε on opposite sides of it. We find C_ε by intersecting δ_e with $A_\varepsilon B_\varepsilon$. Let AB_e be the orthogonal projection of *AB* onto F_A. Then *C* is the intersection of the vertical through C_ε with AB_e, and *S* is the intersection of O_AC with l_e. Joining *A* (resp. *B*) to *S* we find the projection of the geodesic of π on face F_A (resp. F_B).
This construction can be easily drawn on top of the flattened cube, thus dispensing with awkward auxiliary drawings. For instance, if the faces are *F* and *R*, the top view can be drawn on top of face *D* (fig. 3d).
S may or may not be on e (figs. 3c-3e). This, as well as the type of the segments obtained, determines the type of geodesic projection. Below we consider these several cases. Note that we insist that all constructions must be executed within the confines of the paper, that is, of the rectangle that contains the flattened cube. So, in *Case 2.2*, when *S* is outside e, we use an alternative construction to remain within the intended bounds (fig. 3e right). This is a general philosophical principle in spherical perspective: just like the drawing itself, its construction should be compact [Araújo 2016; 2018a].
Case 2.1: *S* is in e (figs. 3c, 3d). Then there is a point P_A on an edge of F_A such that $AS \cap F_A = P_AS$ and a point P_B on an edge of F_B such that $BS \cap F_B = P_BS$. We have two possibilities: If P_A is on the edge of F_A parallel to e, then SP_A crosses parallel edges of the same face, hence we have reduced the problem to a previously solved case, and the projection is the *4-cycle* $SPB\,P^-P_A$. Note that this implies $P_B \equiv P_A^-$ (fig. 3c). If P_A is on an edge adjacent to e, then we have reduced the problem to a previous solved case and the projection is a *6-cycle*, with $P = P_A$ and $Q = S$. This implies that P_B must also be on an edge of F_B adjacent to e, and in fact $P_B = N$. So the *6-cycle* is $P_A\,S\,P_B\,P_A^-\,S^-\,P_B^-$ (fig. 3d).
Case 2.2: *S* is not in e (fig. 3e). Then there are points P_A and Q_A in F_A such that $AS \cap F_A = P_A\,Q_A$ and points P_B and Q_B in F_B such that $BS \cap F_B = P_B\,Q_B$. P_A and Q_A must lie in two edges adjacent to each other, because if these edges were parallel to each other, they would both be perpendicular to e defining a *4-cycle* that would not touch the face where *B* is, but this is absurd since *B* belongs to *g*. Hence P_A and Q_A are on edges adjacent to each other, and the geodesic is the *6-cycle* with $P = P_A$ and $Q = Q_A$, $N = Q_B$, that is, it equals $P_A\,Q_A\,Q_B\,P_A^-\,Q_A^-\,Q_B^-$.

Fig. 3. L.F. Olivero, Geodesics for Case 2, with A and B in different faces: b) Construction of the auxiliary point S; c) P_A is on the edge of F_A parallel to e; d) P_A is on an edge of F_A adjacent to e; e) S is not in e.

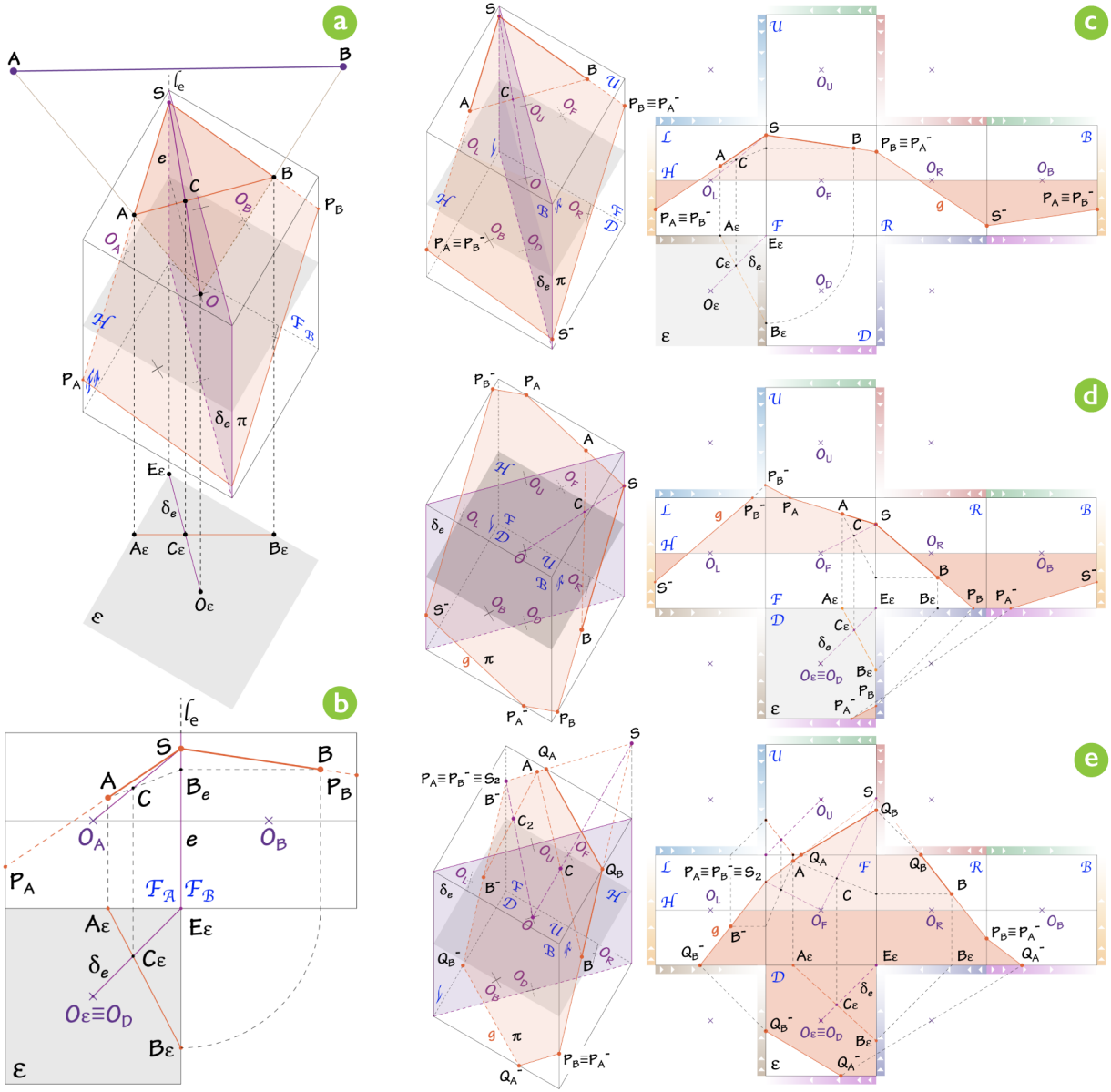

Case 3: Points *A* and *B* are on opposite faces. Then *A* and B^- are on the same face, which reduces the problem to *Case 1*.

Measuring and plotting points

It may surprise the reader that we have plotted antipodes and geodesics from given points, but we haven't said how to plot a particular point. It turns out that it is easier to plot points once we have classified the geodesics. The projection of a generic spatial point *P* is determined by its two characteristic angles λ (longitude or bearing/azimuth) and φ (latitude or elevation), which are the angles one measures when drawing from observation. λ and φ define two *grid-like* geodesics g_λ and g_φ ,that intersect each other at *P* and P^- (fig. 4a). We will find *P* by constructing these geodesics.
Suppose *P* is not on the vertical line through *O* (if it is, then it just projects as O_D or O_U). Let π_λ be the vertical plane through *P* and *O*. π_λ makes an angle λ with the vertical plane through *O* and O_F. Let g_λ be the geodesic of π_λ. π_λ intersects four faces of the cube. Let *I* be one of the faces not touched by g_λ. Then O_I and *P* define a non-vertical *grid-like* geodesic g_φ. The plane of that geodesic π_φ makes an angle φ with *H*.
Construction 2 (geodesic g_λ): let M_{FD} be the midpoint of edge *FD*. Let *J* be the point of the border of *D* such that $M_{FD}\ O_D\ J = \lambda$. The segment $b = O_D\ J$ defines g_λ and we construct it from the two points O_D and *J* as in section *II.3*.
Construction 3 (intersection of g_φ with g_λ): let J_λ be the intersection of g_λ with *H* and *I* the face where J_λ lies. OP intersects the vertical through J_λ at a point P_I. Rotate the triangle $J_\lambda\ OP_I$ around the vertical through J_λ to bring it to face *I*. We obtain a triangle $J_\lambda\ O_H\ P_I$ such that $\angle\ J_\lambda\ O_H\ P_I = \varphi$ and $|\ O_H J_\lambda\ | = |\ b\ |$. If P_I is on face *I*, then $P_I \equiv P$ (fig. 4a right). If is not, then triangle $J_\lambda\ O_H\ P_I$ intersects either the top (resp. bottom) border of face *I* at C_1 and at C_2, where C_1 is on the vertical through J_λ. Let *c* be the segment $C_1\ C_2$. On the top face (resp. bottom) we rotate *c* over the vertical through J_λ. Then the image of *P* will be the point on g_λ such that $|\ C_1\ P\ | = |\ C_1\ C_2\ | = |\ c\ |$ (fig. 4b).
Note that when *I* is the face *B*, it is easier to plot P^- and then use *Construction 1* to get the antipode.

Examples

The constructions of geodesics obtained above allow us to solve any problem in cubical perspective. We will illustrate this with a couple of examples which are generalizations of classical perspective constructions.
Uniform Grids: let us recall and generalize the standard construction of a tiled floor (uniform grid) in classical perspective. Assuming the floor is horizontal and below *O*, and one of the vanishing points of the grid is centred on a face, then we can assume without loss of generality (since the anamorphosis is independent of the cube's size) that face *D* touches the floor. Hence the grid projects on *D* in true size, as an orthogonal grid of horizontals and verticals (fig. 4d) that intersect each horizontal face in uniformly spaced points. These lines can be extended as halves of *grid-like* geodesics, vanishing to O_F, O_L, O_R, O_B. From the bottom left vertex of face *F* we send a diagonal to vanish at the middle point of edge *FR*. We get the exact construction of Piero de La Francesca's uniform grid [Della Francesca 2016, pp. 102, 366]: the 45-degree line intersects each row of lines going to O_F at exactly one point per row, and through these intersections we pass the rows of perpendiculars, to finish the grid. These lines are all *grid-like*, so they extend to points O_R and O_L as seen in *Case I.1* of section *II.3*. The grid can be completed either by symmetry or by using another 45-degre line on face *B* to repeat the construction.
Here, a note is in order. In classical perspective, the location of the vanishing point of the 45-degree line will depend on the distance of the station point to the drawing plane. But in the cubical perspective that is no longer true: although the distance of *O* to the projection plane varies with the size of the cube, the position of the 45-degree vanishing point is invariant. It is always located exactly at the midpoint of edge *FR* (figs. 4d, 4e). The geometric constraint between the various faces of the cube keeps it there, invariant for change of scale. Angles, not linear measurements, determine the cubical drawing. In a way, the cube is just apparent: the underlying structure is that of a sphere. We note that this invariance of the position of the 45-degree vanishing point is at the basis of the method used in [Olivero, Rossi, Barba 2019, p. 59] to plot horizontal and verticals in cubical perspective.
A small diversion may be enlightening. We note that there is a similarity between cubical perspective and the classical device called a *perspective box* [Spencer 2018; Verweij 2010]. If we restrict our attention to a half-space defined by a plane through *O* and parallel to one of the cube's faces, we get a perspective box (fig. 4f) with especially simple symmetry.

Fig. 4. L.F. Olivero, Examples and plotting points. a,b) Image of P using segments b and c; c) Plot of equally distanced elements and VR visualization; d,e) Grid and extended grid construction; f) Uniform grid on a perspective box, made up of half a cube and perspective box example based on [Verweij 2010, p. 61].

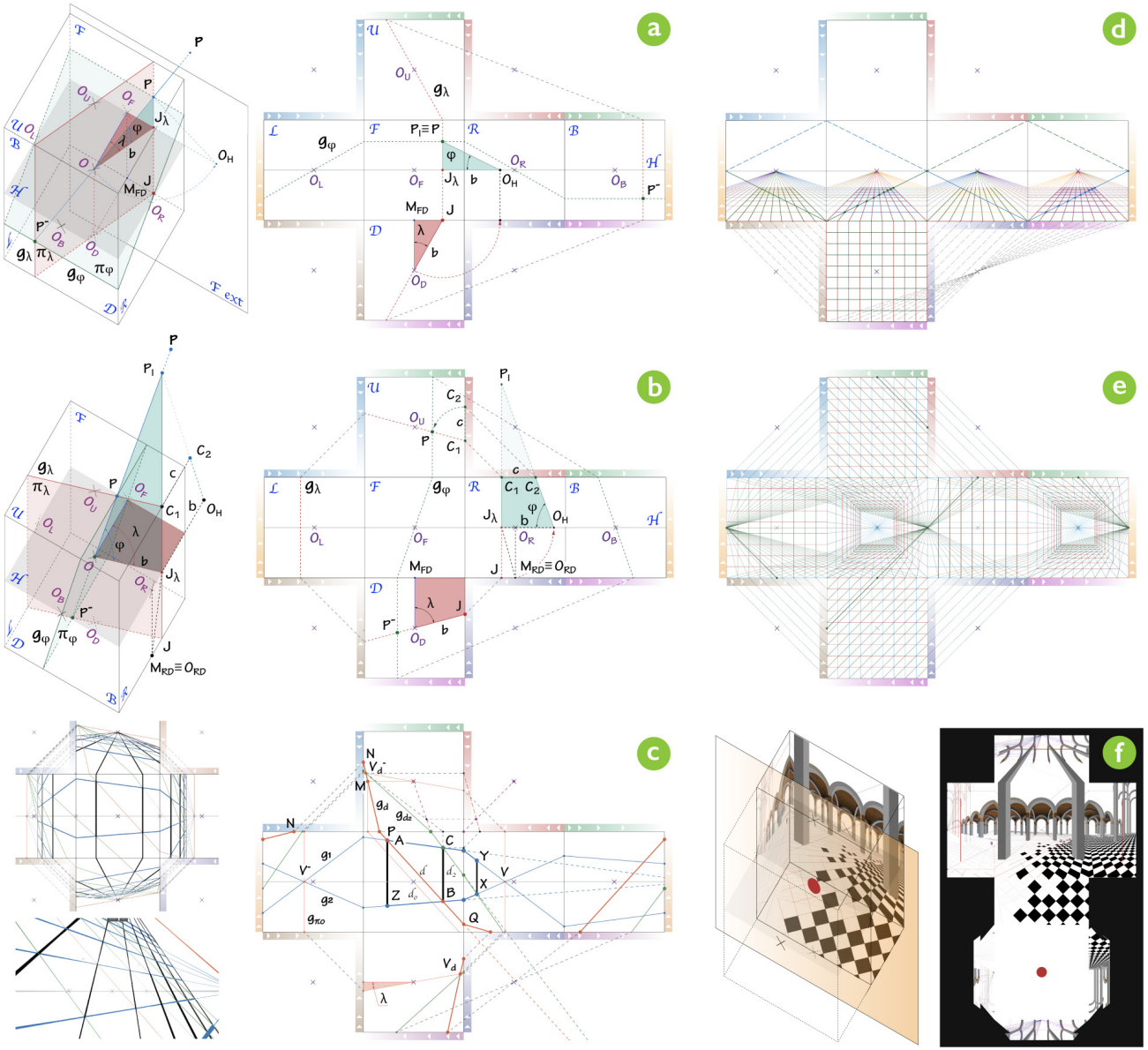

The telephone pole problem: consider now an example involving the plot of equally distanced elements (fig. 4c) from two measured ones. Imagine a scene with equidistant thin columns (e.g. telephone poles) along a vertical plane π that makes an angle with the plane of face *F*. Suppose we measured two points from direct observation and plotted them as in *section III*: point *A* in the upper extreme of the first column and point *B* in the bottom of the second one. Assume also that we measured the angle of π with *F* and we found π to project on face *R* at 10° to the left of O_R. We will show that these three measurements are enough to construct the whole scene.
Following *Case 2* of *section II*, we construct the two geodesics g_1 and g_2 that pass through points *A*,*V* and *B*,*V*. Passing verticals through *A* and *B* we find *Z* on g_2 and *C* on g_1 respectively. Then segments *AZ* and *CB* are the first two columns.
To find the other columns we will define an iterative process based on the vanishing points of the diagonal line $d = AB$. This is a generalization of a well-known construction in classical perspective.
Let g_d be the geodesic of *d*. Since *A* and *B* are in the same face, we construct g_d by *Case 1*. Extending *AB* we get *P* and *Q* in adjacent edges of *F*. Therefore, g_d is a *6-cycle*, and we construct it using points *M* and *N* as in *Case 1.2*. The vanishing set of π is the geodesic $g_{\pi o}$ obtained by translating π to *O*. $g_{\pi o}$ is generated by the vertical on face *R* that passes at 10 degrees to the left of O_R (second case of *1.1.2*) and is a *4-cycle* with segments all disconnected. Because *d* is on π, its vanishing points V_d and V_d^- must be in the vanishing set of π, hence we find them by intersecting g_d with $g_{\pi o}$. We join point *C* with V_d or V_d^- to construct g_{d2} following *Case 2* (in fig. 4c the construction is done above face *R*). Let *X* be the intersection of g_{d2} with g_2. Pass a vertical through *X* to obtain point *Y* on g_1. Segment *XY* defines the third column. We can iterate the process to get as many columns as we like. Since the diagonals go to the same vanishing points, the columns will be equally spaced.
It is important to highlight that in order to construct the same scene using only classical perspective in the plane of the face *F*, the (unique) vanishing point of the diagonals *d*, d_2 and of lines *AC*, *ZD* would be outside of the drawing (by quite a lot in the first case). This worsens without limit as the angle of π with *F* goes to zero. Instead, using geodesics, we draw in a compact way by using whichever of the two vanishing points that happens to be more convenient for the draughtsman. In fact, unlike in classical perspective, we can guarantee that both the vanishing points of a scene and the diagrams required for their construction are within the bounds of the drawing.
In (fig. 1a) we have an elaborate example of both the uniform tiling of the previous section and of the present construction with regard to the columns. The column multiplication is in that case simplified, since π will be parallel to face *F* and the vanishing points of the diagonals of the columns will lie on face *R* and *L* rather than *U* and *D*.

Conclusions

Each spherical perspectives, just like each cartographic map, and exactly for the same reasons, has its positive and negative aspects. Cubical perspective is no exception. Its positive aspects, when compared to the other main contenders –equirectangular and azimuthal equidistant perspectives– are clear: it works as a classical perspective in each face, and therefore requires much less effort from the user's intuition. Also, if classical perspective can be characterized as the single spherical perspective that is still an anamorphosis [Araújo 2018a], hence retains the property of mimesis, then cubical perspective holds a close second place, being a set of six local anamorphoses. Finally, from the point of view of construction, unlike the other two contending perspectives, we have shown that we can construct all geodesic segments from the angular measurements of two given points by descriptive geometry diagrams. In both the azimuthal equidistant and equirectangular cases [Araújo 2018b; Barre, Flocon, Bouligand 1967] this can only be done with the measurement of specially chosen points which may sometimes be inconvenient to measure. Further, this construction is exact, without requiring approximations or interpolations, due to its linearity. As for negative points, the main one is the enumeration of cases that we had to go through in this solution, that is comparatively complex when set up against the other two perspectives and the sometimes troublesome process of dealing with the discontinuities from one face to another [Olivero, Sucurado 2019, p. 57]. The abrupt changes of plane reflect themselves in a comparative inelegance of construction, unseen in the curvilinear cases. All in all, cubical perspective, when treated properly as a spherical perspective, must hold an important place in the growing bestiary of immersive perspectives from which the architect, artist and engineer can choose according to their needs.

Acknowledgements
This work is an advancement of a PhD thesis in "Environment, Design and Innovation" titled "Hybrid Immersive Models from Autographic Sketches" by L.F. Olivero and funded by University of Campania "Luigi Vanvitelli", with A.B. Araújo (Universidade Aberta - Portugal) as the international advisor, funded by FCT national funds through project UID/Multi/04019/2013 and A. Rossi (Department of Engineering, University of Campania "Luigi Vanvitelli") as advisor.

Authors

António Bandeira Araújo, Department of Sciences and Technology, Universidade Aberta and CIAC, antonio.araujo@uab.pt
Lucas Fabián Olivero, Engineering Department, University of Campania "Luigi Vanvitelli", lucasfabian.olivero@unicampania.it
Adriana Rossi, Engineering Department, University of Campania "Luigi Vanvitelli", adriana.rossi@unicampania.it

Reference List

Araújo, A.B. (2016). Topologia, anamorfose, e o bestiário das perspectivas curvilíneas. In *Convocarte: revista de ciências da arte. Arte e geometria*, No. 2, pp. 51-69.

Araújo, A.B. (2018a). Ruler, compass, and nail: Constructing a total spherical perspective. In *Journal of Mathematics and the Arts*, Vol. 12, No. 2-3, pp. 144–169. https://www.doi.org/10.1080/17513472.2018.1469378.

Araújo, A.B. (2018b). Drawing Equirectangular VR Panoramas with Ruler, Compass, and Protractor. In *Journal of Science and Technology of the Arts*, Vol. 10, No. 1, pp. 15-27. https://www.doi.org/10.7559/citarj.v10i1.471

Araújo, A.B., Olivero, L.F., Rossi, A. (2019). Boxing the Visual Sphere: Towards a systematic solution of the cubical perspective. In P. Belardi (ed.). *REFLECTIONS the Art of Drawing. the Drawing of Art*, pp. 33-40. Roma: Gangemi Editore. https://www.doi.org/10.36165/1004.

Arnheim, R. (1954). *Art and Visual Perception. A psychology of the creative eye*. Berkeley-Los Angeles: University of California Press.

Barba, S., Fiorillo, F., Naddeo, A. (2014). Tecniche di image editing: Un possibile 'work flow' per le architetture prospettiche. In Valenti, G.M. (a cura di). *Prospettive architettoniche. Conservazione digitale, divulgazione e studio*, Vol. I, pp. 871-886. Roma: Sapienza Università Editrice.

Barba, S., Rossi, A., Olivero, L.F. (2018). CubeME, a variation for an immaterial rebuilding. In R. Salerno (a cura di). *Rappresentazione / Materiale / Immateriale. Drawing as (in)Tangible Representation*, pp. 31-36. Roma: Gangemi Editore.

Barre, A., Flocon, A., Bouligand, G. (1967). *La Perspective curviligne: De l'espace visuel à l'image construite*. Paris: Flammarion.

Cabezos Bernal, P.M., Cisneros Vivó, J.J. (2016). Panoramas esféricos estereoscópicos. In *EGA Expresión Gráfica Arquitectónica*, No. 21 (28), pp. 70-81. https://doi.org/10.4995/ega.2016.6264.

Della Francesca, P. (2016). *De prospectiva pingendi*. a cura di C. Gizzi. Venezia: Ca' Foscari-Digital Publishing (First ed. 1474). https://www.doi.org/10.14277/978-88-6969-099-0.

García-García, C., Galán Serrano, J., Arce Martínez, J.M. (2016). The hybrid drawing as a way of architectural representation. In F.F. Miralles, et al. (eds.), *Dibujar, Construir, Soñar. Drawing, Building, Dreaming*, pp. 1037-1049. Valencia: Tirant lo Blanch.

Olivero, L.F., Rossi, A., Barba, S. (2019). A codification of cubical projection for the generation of immersive models. In *Diségno*, No. 4, pp. 53-63. https://www.doi.org/10.26375/disegno.4.2019.07.

Olivero, L.F., Sucurado, B. (2019). Analogical immersion: Discovering spherical sketches between subjectivity and objectivity. In *ESTOA. Revista de la Facultad de Arquitectura y Urbanismo de la Universidad de Cuenca*, Vol. 8, No. 16, pp. 47-59. https://www.doi.org/10.18537/est.v008.n016.a04.

Rossi, A. (2017). *Immersive high resolution photographs for cultural heritage*. Vol. 2. Padova: libreriauniversitaria.it

Schön, D.A. (2017). *The Reflective Practitioner: How Professionals Think in Action*. London: Routledge. https://www.doi.org/10.4324/9781315237473.

Spencer, J. (2018). Illusion as ingenuity. Dutch perspective boxes in the Royal Danish Kunstkammer's 'Perspective Chamber'. In *Journal of the History of Collections*, Vol. 30, No. 2, pp. 187-201. https://www.doi.org/10.1093/jhc/fhx024.

Tran Luciani, D., Lundberg, J. (2016). Enabling Designers to Sketch Immersive Fulldome Presentations. In *Proceedings of the 2016 CHI Conference Extended Abstracts on Human Factors in Computing Systems*, pp. 1490-1496. https://doi.org/10.1145/2851581.2892343.

Verweij, A. (2010). Perspective in a box. In *Nexus Network Journal*, Vol. 12, No. 1, pp. 47-62. https://www.doi.org/10.1007/s00004-010-0023-7.